Electrical Resistivity Measurements on Manganese Oxides with Layer and Tunnel Structures: Birnessites, Todorokites, and Cryptomelanes

Roberto N. De Guzman,[†] Amir Awaluddin,[†] Yan-Fei Shen,[†] Zheng Rong Tian,[†] Steven L. Suib,*[,†,‡] Stanton Ching,*[,§] and Chi-Lin O'Young*[,⊥]

Charles E. Waring Laboratory, Department of Chemistry, U-60, University of Connecticut, Storrs, Connecticut 06269-3060; Institute of Materials Science and Department of Chemical Engineering, University of Connecticut, Storrs, Connecticut 06269-3060; Department of Chemistry, Connecticut College, New London, Connecticut 06320; and Texaco Research Center, Texaco Inc., P.O. Box 509, Beacon, New York 12508

Received September 13, 1994. Revised Manuscript Received April 27, 1995[⊗]

Direct-current measurements were used to determine the electrical resistivities of several manganese oxide materials having either layered or tunnel structures. Birnessite (Na-OL-1, OL = octahedral layer) consists of layers of edge- and corner-sharing MnO_6 octahedral units with Na^+ in the interlayer regions. Todorokite and cryptomelane (Mg-OMS-1 and K-OMS-2, respectively, OMS = octahedral molecular sieve) are similarly built from MnO_6 units, but in these systems the octahedra join to form 6.9 and 4.6 Å tunnels occupied by Mg^{2+} and K^+, respectively. Resistivities were also measured for OL-1, OMS-1, and OMS-2 materials in which (a) cation exchange was carried out at layer and tunnel sites or (b) isomorphous substitution for Mn was performed by doping small amounts of foreign cations into the manganese oxide framework. Four probe measurements on pressed pellets reveal that OL-1 and OMS-1 materials have resistivities on the order of 10^5–10^6 Ω cm at 298 K. OMS-2 materials have resistivities in the range 10^5–10^6 Ω cm at 298 K. Variable-temperature measurements establish a general pattern of increasing resistivity with decreasing temperature. However, between 153 and 293 K, OL-1 and OMS-1 materials do not obey a simple exponential variation of resistivity and temperature. By contrast, OMS-2 samples follow the Arrhenius relationship over a comparable temperature range. Activation energies for the conductivity OMS-2 materials were calculated to be in the range 0.5–0.6 eV. Solid-state voltammetry was used to determine the electrical resistance of OMS-1 and OMS-2 samples at higher temperatures from 298 to 673 K. A general exponential decrease in resistance with increasing temperature was observed for both classes of materials. Ac resistivity measurements show similar trends to dc resistivity data.

Introduction

The electrical resistivity of manganese oxides has attracted significant interest due to the wide spread use of common manganese dioxides in secondary batteries.[1–5] Electrical properties have also been studied for related materials such as titanium cryptomelanes,[6] mixed manganese–iron oxides,[7] nickel–manganite,[8] and hausmannite (Mn_3O_4).[9,10] In addition, the resistivity change for the bixbyite (Mn_2O_3) to hausmannite (Mn_3O_4) phase transformation at high temperature has been reported.[11]

Electrical properties have been determined for the tunnel-containing manganese oxide, cryptomelane, and data for both single crystals and powders are available.[12] Single crystals of cryptomelane with a composition of $K_{1.33}Mn_8O_{16}$ were prepared electrolytically at 505 °C.[12,13] Direct-current measurements revealed them to be semiconducting with resistivity (ϱ) values of 33 Ω cm at 21 °C and 2.5 Ω cm at 80 °C. Powdered cryptomelane samples were prepared by reduction of $KMnO_4$ with HCl at 80 °C followed by leaching in boiling 3 M HNO_3. Resistivities of pelletized samples were determined with ac techniques and ϱ values were found to be 4.3×10^4 Ω cm at 35 °C and 5.9×10^2 Ω cm at 94 °C. The resistivity of a layered manganese oxide, Na–birnessite,

[†] Department of Chemistry, University of Connecticut.
[‡] Institute of Materials Science and Department of Chemical Engineering, University of Connecticut.
[§] Connecticut College.
[⊥] Texaco Inc.
* To whom correspondence should be addressed.
[⊗] Abstract published in *Advance ACS Abstracts,* June 1, 1995.

(1) Strobel, P.; Charenton, J. C. *Rev. Chim. Mineral.* **1986**, *23*, 125–137.
(2) Euler, K. J.; Mueller-Helsa, H. *J. Power Sources* **1979**, *4*, 77–89.
(3) Ruetschi, P. *J. Electrochem. Soc.* **1984**, *131*, 2737–2744.
(4) Ruetschi, R.; Giovanoli, R. *J. Electrochem. Soc.* **1988**, *135*, 2663–2669.
(5) Voinov, M. *J. Electrochem. Soc.* **1981**, *128*, 1822–1823.
(6) Yoshikado, S.; Ohachi, T.; Taniguchi, I.; Onoda, Y.; Watanabe, M.; Fujiki, Y. *Solid State Ionics* **1983**, *9–10*, 1305–1310.
(7) Pattanayak, J. *J. Mater. Sci. Lett.* **1991**, *10*, 1461–1464.
(8) Sarkar, S. K.; Sharma, M. L.; Bhaskar, H. L.; Nagpal, K. C. *J. Mater. Sci.* **1984**, *19*.
(9) Logothetis, E. M.; Park, K. *Solid State Commun.* **1975**, *16*, 909–912.
(10) Metselaar, R.; Van Tol, R. E. J.; Piercy, P. *J. Solid State Chem.* **1981**, *38*, 335–341.
(11) Pattanayak, J.; Rao, V. S.; Maiti, H. S. *J. Mater. Sci. Lett.* **1989**, *8*, 1405–1407.
(12) Strobel, P.; Vicat, J.; Qui, D. T. *J. Solid State Chem.* **1984**, *55*, 67–73.
(13) Vicat, J.; Fanchon, E.; Strobel, P.; Qui, D. T. *Acta Crystallogr.* **1986**, *B42*, 162–167.

0897-4756/95/2807-1286$09.00/0

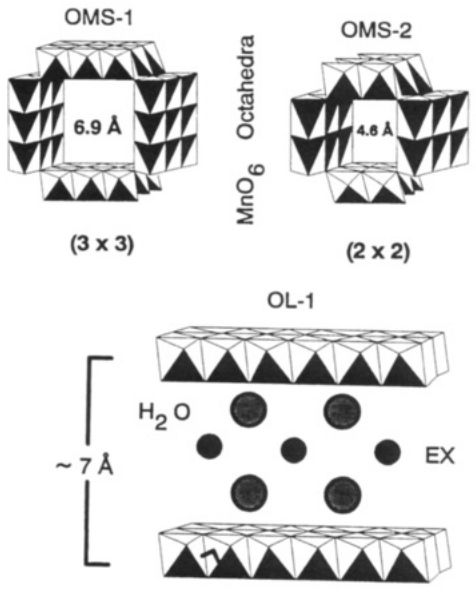

Figure 1. Structures of synthetic todorokite (OMS-1), cryptomelane (OMS-2) octahedral molecular sieves and birnessite (OL-1) octahedral layer. Smaller solid spheres = exchangeable (Ex) cations; larger hatched spheres = interlayer H_2O molecules.

was also determined by ac methods and a ϱ value of 4.8×10^5 Ω cm was measured at 27 °C.[14]

We recently reported new syntheses of manganese oxides with layer and tunnel structures. The basic building blocks of these materials are MnO_6 octahedra that are interconnected by edge- and corner-shared sites. Octahedral molecular sieves (OMS) have been prepared with todorokite (OMS-1)[15,16] and cryptomelane (OMS-2)[17] tunnel structures, while octahedral layer (OL) solids have been synthesized with the birnessite structure (OL-1, Figure 1). Although these materials are primarily composed of MnO_6 units, the tunnel and interlayer sites can be occupied by other metal cations. The type of cation can be controlled somewhat for OL-1 through cation exchange. In particular, Na^+ in Na-OL-1 can be exchanged for a variety of alkali, alkaline earth, and transition metal cations. Similar control is available for OMS-1 since several M-OL-1 materials (M = Mg^{2+}, Co^{2+}, Ni^{2+}, Cu^{2+}, and Zn^{2+}) are OMS-1 precursors.[16] By contrast, K^+ cations that occupy the tunnels of cryptomelane are not readily ion exchanged, but different synthetic strategies have been used to incorporate cations such as Ba^{2+} and Pb^{2+}. All three types of manganese oxides have been identified as naturally occurring minerals. Interest in these substances comes from their potential use as heterogeneous catalysts and as cathode materials for secondary batteries.

Despite a growing body of work on the electrical properties of manganese oxides, no resistivity data are available for OMS-1 and cation-exchanged OL-1 materials. The effect of isomorphous cation doping into the manganese oxide framework is also unexplored. Our work on the electrical properties of these materials has thus far been limited to an electrochemical study using carbon paste composites of OMS-1 and OMS-2.[18] In this work, the electrical resistivities of synthetic birnessite (OL-1), todorokite (OMS-1), and cryptomelane (OMS-2) were determined by different methods in two temperature regimes. Low-temperature resistivities were measured using the four probe, or the van der Pauw,[19,20] method from 293 to 153 K. High-temperature resistivities between 293 and 673 K were determined voltammetrically using a solid-state cell. Significantly, it was possible to examine the effect of cation substitution in the layers of OL-1 and in the tunnels of OMS-1. The influence of small amounts of transition metal dopants into the manganese oxide framework was also explored. The primary motivation for this research was to measure the conductive properties of synthetic manganese oxides and to determine how the conductivity of these materials might be influenced by cation exchange (in tunnel and layer sites) and isomorphous cation substitution (doping in the manganese oxide framework).

Experimental Section

Sample Preparation. OL-1,[21,22] OMS-1,[15,16] and OMS-2[17] materials were synthesized from literature procedures. Samples weighing about 0.3 g were pressed into 1-mm thick disks with 13-mm diameters using an applied pressure of 52 000 psi for 3 min. Sample holders were prepared from 2.5-cm-diameter plastic vial caps. Conductive silver epoxy (ACME Conductive Adhesives, Allied Products Corp., New Haven, CT) was used to provide electrical contact with copper wires. The manganese oxide discs with their attached wires were then secured in the sample holder by filling lower portion with epoxy resin (Epo-Mix Epoxide, Buehler, Lake Bluff, IL) which provided mechanical stability for the contacts (Figure 2A).

Low-Temperature Resistivity. Keithley 136A multimeters were used for current and voltage measurements. A Keithley 480 picoammeter was used for more resistive samples. A home-built dc power supply with voltage output of 0−5 V was used. The circuit configuration for determining resistivity is shown in Figure 2B. A home-built switchbox was assembled to measure R_1, R_2, R_3, and R_4 sequentially without physically moving the sample. The resistivity was calculated using the formula in eq 1,[19,20] where ϱ is the resistivity in Ω cm, W is

$$\varrho = \frac{\pi W}{\ln 2}\left(\frac{R_1 + R_2}{2}\right) f\left(\frac{R_1}{R_2}\right) \qquad (1)$$

the disk thickness, V_{AB} is the voltage measured across contacts A and B, and I_{CD} is the current across contacts C and D (Figure 2B). The factor f depends on the ratio R_1/R_2 and can be determined as in eq 2,[19,20] where Q is R_1/R_2. A computer

$$\frac{Q-1}{Q+1} = \frac{f}{\ln 2}\cosh^{-1}\left[\frac{1}{2}\exp\left(\frac{\ln 2}{f}\right)\right] \qquad (2)$$

program[23] written in Pascal was used to calculate resistivities from eqs 1 and 2. Activation energies (E_g) were determined from the Arrhenius relationship, eq 3,[24] where A is the

(14) Charenton, J. C.; Strobel, P. *Solid State Ionics* **1987**, *24*, 333−341.
(15) Shen, Y. F.; Zerger, R. P.; Suib, S. L.; McCurdy, L.; Potter, D. I.; O'Young, C. L. *J. Chem. Soc., Chem. Commun.* **1992**, 1213−1214.
(16) Shen, Y. F.; Zerger, R. P.; De Guzman, R. N.; Suib, S. L.; McCurdy, L.; Potter, D. I.; O'Young, C. L. *Science* **1993**, 511−515.
(17) De Guzman, R. N.; Shen, Y. F.; Neth, E. J.; Suib, S. L.; O'Young, C. L.; Levine, S.; Newsam, J. M. *Chem. Mater.* **1994**, *6*, 815−821.
(18) De Guzman, R. N.; Shen, Y. F.; Shaw, B. R.; Suib, S. L.; O'Young, C. L. *Chem. Mater.* **1993**, *5*, 1395−1400.
(19) Van Der Pauw, L. J. *Phillips Res. Rep.* **1958**, *13*, 1−9.
(20) Van Der Pauw, L. J. *Phillips Tech. Rev.* **1958/59**, *20*, 220−224.
(21) Golden, D. C.; Chen, C. C.; Dixon, J. B. *Clays Clay Miner.* **1987**, *35*, 271−280.
(22) Chen, C. C.; Golden, D. C.; Dixon, J. B. *Clays Clay Miner.* **1986**, *34*, 564−571.
(23) De Guzman, R. M.S. Thesis, University of Connecticut, 1994.
(24) Cox, P. A. *The Electronic Structure and Chemistry of Solids*; Oxford University Press: Oxford, 1987.

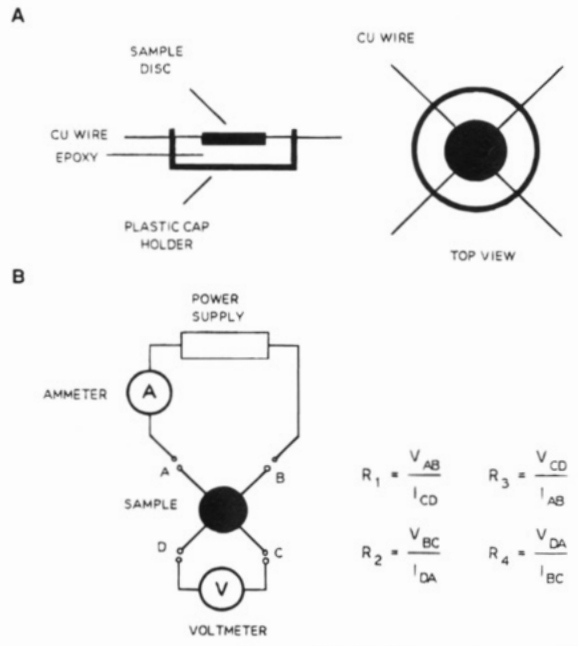

Figure 2. (A) Sample cell and holder for four-probe resistivity measurements. (B) Circuit diagram for four-probe measurements.

$$\sigma = A \exp\left(\frac{-E_g}{kT}\right) \tag{3}$$

preexponential factor, T is the absolute temperature, and k is the Boltzmann constant (8.616×10^{-5} eV/K). For semiconductors, linear plots of log R vs $1/T$ have slopes directly related to E_g.

Resistive heating of the samples was minimized by passing currents of no more than 0.1 mA. Temperature was monitored using an Omega digital thermometer with a J-type thermocouple positioned less than 5 mm from the disk. Suitable temperature control between 153 and 293 K was achieved by varying the height of the sample cell above a pool of liquid nitrogen in a Dewar flask. For most samples, the data points obtained on cooling and heating the sample cell traced the same curve. In the few cases in which cooling and heating data showed small deviations, averages of the resistivities were plotted.

High-Temperature Resistivity. Solid-state voltammetry was used to determine the electrical resistance of manganese oxides from 293 to 673 K. Measurements were obtained with a solid-state cell which was modified from a design taken from the literature,[25,26] Figure 3A. Platinum foil electrodes (3×10 mm) were cleaned prior to each use by dipping in nitric acid, sonication in water for 5 min, and thorough rinsing with distilled deionized water. The Pt electrodes were placed on the sample disk and held in place with glass and aluminum plates as shown in Figure 3A. Silver wire was used to connect the Pt electrodes to a BAS 100A electrochemical analyzer. The entire cell was enclosed in a test tube and argon or nitrogen gas passed over it at about 80 cm^3/min. The heating rate was regulated using an Omega temperature controller with the thermocouple positioned less than 5 mm from the sample disk. A schematic of the experimental setup is shown in Figure 3B.

Ac Resistivity Measurements. Ac resistivity measurements were done by attaching leads across opposite sides of a 0.1 g pellet of manganese oxide material with small amounts of silver epoxy. Ac resistivity measurements were done at low frequency (1 kHz). In this case, the following relationship holds:

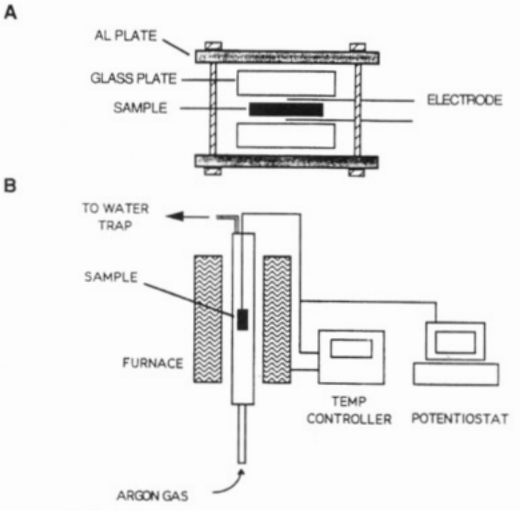

Figure 3. (A) Solid-state cell for high-temperature resistance measurements. (B) Experimental setup for the voltammetric determination of resistance from 293 to 673 K.

$$1/Z = 1/R + 1/R_c \tag{4}$$

At low frequency, R_c is large and the relationship simplifies to eq 5.

$$1/Z \sim 1/R \tag{5}$$

An LCR Meter Model LCR-745G ac impedance instrument was used for all ac resistivity measurements. Measurements were done by connecting the low current and low potential leads to one face of the pressed pellets and the high current and high potential leads to the opposite face of the pellet.

Results and Discussion

The resistivities determined for birnessite (OL-1), todorokite (OMS-1), and cryptomelane (OMS-2) samples with four probe measurements are summarized in Table 1. Resistivities obtained from pressed pellets of powdered samples such as these are inherently dominated by interparticle grain boundary resistance. Consequently, resistivity values obtained from pressed powders are typically 2–3 orders of magnitude greater than their single-crystal counterparts.[27] The measurements are also averaged over all crystallographic orientations, which is an important consideration for materials that exhibit anisotropic conduction. Given these inherent conditions, judgments concerning the absolute bulk resistivities of OL-1, OMS-1, and OMS-2 materials are unlikely to be valid. However, relative comparisons among the different manganese oxides are probably justified due to their similarity in composition and structure.[28] Pressed pellets of OL-1, OMS-1, and OMS-2 were examined using scanning electron microscopy to compare differences in surface morphology between these samples. The surfaces of OL-1 and OMS-1 pellets are virtually identical with magnification up to 10 000×. Pellets of OMS-2 were are also similar to those of OL-1 and OMS-1, though OMS-2 surfaces have a somewhat more grainy appearance. The influence of an external force on the pressed pellets was assessed by measuring

(25) Susic, M.; Petranovic, N. *Electrochim. Acta* **1978**, *23*, 1271–1274.
(26) Susic, M. *Electrochim. Acta* **1979**, *24*, 535–540.
(27) Coleman, L. *Rev. Sci. Instrum.* **1978**, *49*, 58–62.
(28) (a) Gutman, F.; Lyons, L. *Organic Semiconductors*; Wiley: New York, 1967. (b) *Handbook of Conducting Polymers*; Skotheim, T. A., Ed.; Marcel Dekker: New York, 1986. (c) Collman, J. P.; McDevitt, J. T.; Leidner, C. R.; Yee, G. T.; Torrance, J. B.; Little, W. A. *J. Am. Chem. Soc.* **1987**, *109*, 4606–4614.

Table 1. Resistivities of Birnessites (OL-1), Todorokites (OMS-1), and Cryptomelanes (OMS-2)

sample	ϱ (Ω cm, 298 K)	ϱ (Ω cm, 273 K)	ϱ (Ω cm, 173 K)
Na-OL-1	5.2×10^5	1.4×10^6	2.7×10^6
Cu-OL-1 (F)[a]	1.2×10^6	1.8×10^6	5.0×10^6
Cu-OL-1 (L)[b]	3.3×10^5	8.4×10^5	3.9×10^6
Mg-OMS-1	3.6×10^5	8.3×10^5	1.9×10^6
Cu-OMS-1 (F)	1.3×10^6	1.5×10^6	1.7×10^6
Cu-OMS-1 (T)[c]	1.6×10^5	4.5×10^5	2.5×10^6
K-OMS-2 (r)[d]	4.4×10^2	1.0×10^3	2.1×10^4
K-OMS-2 (c)[d]	2.6×10^3	2.3×10^3	6.0×10^4
Cu-OMS-2	8.3×10^2	2.2×10^3	5.6×10^4

[a] (F) refers to Cu^{2+} ions in the framework structure. [b] (L) refers to Cu^{2+} ions in interlayer sites of OL-1. [c] (T) refers to Cu^{2+} ions in the tunnel sites of OMS-1. [d] K-OMS-2 (r) from reflux; K-OMS-2 (c) from calcination.

the room-temperature resistivity of manganese oxide samples under pressure.[29] It was found that resistivities for Na-OL-1, Mg-OMS-1, and K-OMS-2 were unchanged when measured under pressures of up to 100 psi.

The OL-1 and OMS-1 pressed pellets have room-temperature resistivities in the range 10^5-10^6 Ω cm. OMS-2 samples have resistivities of 10^2-10^3 Ω cm. The data indicate that these manganese oxides are semiconductors. This assessment gains qualitative support from scanning electron microscopy experiments which show only mild charging from these samples. All manganese oxide samples exhibit a general trend toward higher resistivities at low temperatures, as expected of semiconductors. However, this trend was not rigorously upheld for some OL-1 and OMS-1 samples at low temperature. Indeed, in a few cases the resistivity decreased as the temperature was lowered. OMS-2 materials showed the greatest resistivity variation among the different manganese oxides from 273 to 173 K. Resistivities of OMS-2 samples increased by 2 orders of magnitude in this temperature range whereas resistivities of OL-1 and OMS-1 samples increased by 1 order of magnitude.

Humidity was found to have a varying effect on manganese oxide resistivities. Measurements on OMS-2 samples showed less than 5% decrease in resistivity upon changing from a dry nitrogen atmosphere to water-saturated air at 27 °C. Under the same conditions, OMS-1 materials show a slightly larger decrease of 10–20%. The largest changes were observed for OL-1 samples, which experienced resistivity decreases of 40–50% in going from dry nitrogen to water-saturated air at 27 °C. Given that most measurements made in this study were carried out over an undisturbed pool of liquid nitrogen, humidity control was considered unnecessary and the ambient atmosphere around the manganese oxide pellets was assumed to be relatively free of moisture. This presumption appears justified since resistivity values of Na-OL-1 were found to be in close agreement with previously reported results obtained under 0% humidity.[14]

Birnessites (OL-1). Figure 4 shows the general increase in resistivity of Na–birnessite (Na-OL-1) with decreasing temperature from 293 to 163 K. The plot shows two unusual humps centered at ϱ values of 2.3×10^6 Ω cm (243 K) and 3.5×10^6 Ω cm (198 K). The resistivities of two types of Cu–birnessites (Cu-OL-1)

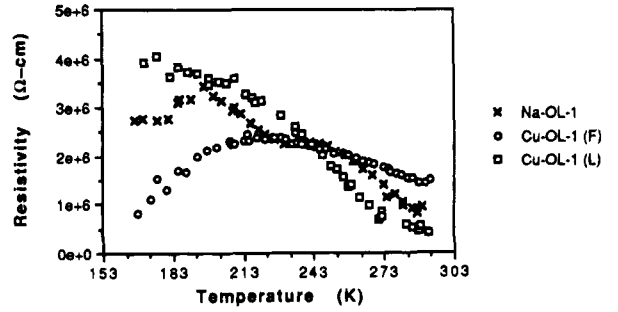

Figure 4. Low-temperature resistivity of birnessites (OL-1).

are also shown in Figure 4. Cu-OL-1(F) refers to Na-OL-1 with small quantities of Cu^{2+} isomorphously substituted for Mn in the Na-OL-1 framework. The Cu-OL-1(F) was prepared by introducing Cu^{2+} ions during the oxidation of Mn^{2+} solution in the synthesis of Na-OL-1. This procedure produces Cu-OL-1(F) with metal atom percentages for Cu of 1–2%. The resistivity of Cu-OL-1(F) showed a broad peaklike response with a maxima at 223 K having a ϱ value of 2.5×10^6 Ω cm. This unusual plot suggests a poorly defined semiconductor-to-metal transition, though we have no explanation for such as an occurrence in this material. In Cu-OL-1(L), the interlayer sites of birnessite are occupied by Cu^{2+}. These samples were prepared by cation exchange using Na-OL-1 in a stirred solution of Cu^{2+}. The resistivity of Cu-OL-1(L) increased with decreasing temperature. The ϱ vs T plot shows a slight sigmoidal shape. Judging from the plot in Figure 4, it appears that the introduction of Cu^{2+} ions into the manganese oxide framework of OL-1 materials has a significant effect on the resistive behavior. The effect seems particularly strong since the level of Cu^{2+} doping is relatively low. Plots of log resistivity vs reciprocal temperature for all three materials exhibited linear Arrhenius plots from about 290 to 250 K. Below this temperature region, the data show significant variation. Manganese oxide resistivity has not previously been studied at these low temperatures and information about phase transformations and other phenomena are unavailable for interpreting the deviations from Arrhenius behavior. Activation energies (E_g) were calculated for the three birnessites in the temperature region from 290 to 250 K, and the results are listed in Table 2. Values of E_g for Na-OL-1 (0.78 eV) and Cu-OL-1(L) (0.88 eV) are not substantially different and compare favorably with E_g values reported previously for sodium and potassium birnessites. (0.96 and 0.98 eV, respectively, determined between 298 and 323 K).[14] By contrast, Cu-OL-1(F) has a significantly lower E_g of 0.26 eV. This difference may reflect a large influence on birnessite resistivity from low levels of Cu^{2+} doped into the manganese oxide framework.

Todorokites (OMS-1). Resistivity has previously not been measured for todorokites. Pure materials have been synthesized only recently.[15,16] Todorokites were found to have similar resistivities to birnessites and values for OMS-1 materials ranged from 10^5 to 10^6 Ω cm regardless of whether different divalent cations were exchanged into the tunnel sites (OMS-1(T)) or isomorphously doped into the manganese oxide framework (OMS-1(F)). Table 1 lists resistivities for Mg-OMS-1, Cu-OMS-1(F), and Cu-OMS-1(T). In these systems, Mg-OMS-1 and Cu-OMS-1(T) represent OMS-1 with Mg^{2+}

(29) Interrante, L. V., personal communication.

Table 2. Activation Energies of OL-1, OMS-1, and OMS-2[a]

sample	temp range (K)		E_g(eV)
	Low Temperature		
Na-OL-1	260	289	0.78
Cu-OL-1 (F)	256	293	0.26
Cu-OL-1 (L)	250	292	0.88
Mg-OMS-1	252	294	0.66
Cu-OMS-1 (F)	252	286	0.38
Cu-OMS-1 (T)	252	286	0.84
K-OMS-2 (r)	166	290	0.50
K-OMS-2 (c)	214	290	0.58
Cr-OMS-2	158	296	0.58
Cu-OMS-2	166	256	0.52
Ni-OMS-2	159	256	0.58
	High Temperature		
Mg-OMS-1	318	578	1.54
Cu-OMS-1 (F)	438	673	1.40
Cu-OMS-1 (T)	309	673	2.40
K-OMS-2 (r)	299	673	1.24
Cu-OMS-2	308	583	1.50

[a] See Table 1 for abbreviations.

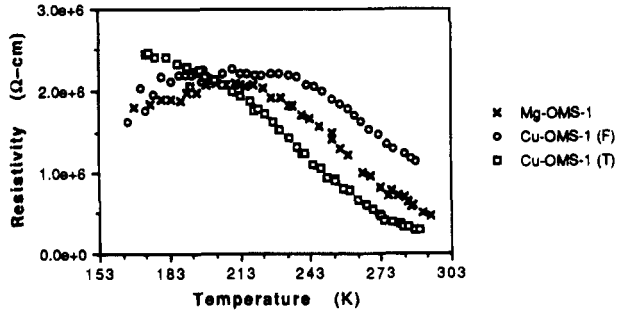

Figure 5. Low-temperature resistivity of todorokites (OMS-1).

and Cu^{2+} as the tunnel cations. These materials were prepared from Na-OL-1 by initial cation exchange with Mg^{2+} or Cu^{2+} followed by autoclave treatment at 150–160 °C to generate Mg-OMS-1 and Cu-OMS-1, respectively. Cu-OMS-1(F) was obtained by (a) carrying out isomorphous framework substitution in Na-OL-1 as describe above for the Cu-OL-1(F) birnessite, (b) cation exchange of Mg^{2+} for interlayer Na^+, and (c) autoclave treatment at 150–160 °C. The resulting Cu-OMS-1(F) has Mg^{2+} in the tunnels and 1–2% Cu^{2+} isomorphously substituted in the manganese oxide framework. Resistivities were also measured at room temperature for similar todorokites with divalent transition metals as either tunnel cations or low-level framework dopants. The resistivity values for Co-OMS-1, Ni-OMS-1, and Zn-OMS-1 fell in the same range as the OMS-1 materials are listed in Table 1.

Variable temperature data for Mg-OMS-1, Cu-OMS-1(F), and Cu-OMS-1(T) are shown in Figure 5. As with the OL-1 manganese oxides, the OMS-1 materials exhibit unusual low-temperature behavior. In particular, ϱ vs T plots for Mg-OMS-1 and Cu-OMS-1(F) have the same broad, arching feature that was observed in the ϱ vs T plot for Cu-OL-1(F). As discussed previously for birnessites, such low-temperature data indicate some sort of semiconductor-to-metal transition, but the origin of the phenomenon is unknown.

Similarities in electrical properties between OMS-1 and OL-1 materials also extend to thermal activation. As noted previously in OL-1 materials, framework doping in OMS-1 appears to have a noticeable effect in lowering E_g for the temperature range above 250 K,

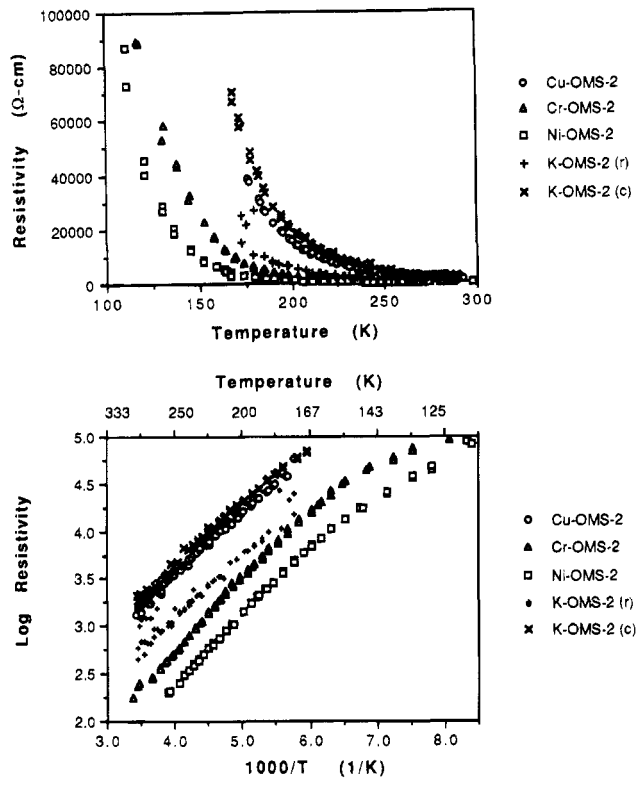

Figure 6. (A, top) Low-temperature resistivity of cryptomelanes (OMS-2). (B, bottom) Arrhenius plots.

Table 2. The E_g values of 0.66 eV for Mg-OMS-1 and 0.84 eV for Cu-OMS-1(T) are significantly higher than the E_g of 0.38 eV for Cu-OMS-1(F). Again, the low level of Cu^{2+} doping into the manganese oxide framework apparently has a strong influence on thermal activation for conduction. Since there was uncertainty about the conduction mechanism at temperatures below <250 K, activation energies were not evaluated in this range.

Cryptomelanes. The effects of temperature on the resistivity of different OMS-2 materials are shown in Figures 6A and 6B. OMS-2 samples followed an exponential increase in resistivity with decreasing temperature. In these systems, OMS-2 refers to materials with K^+ in the tunnels. Samples were produced by refluxing of acidic solutions of Mn^{2+} and $KMnO_4$.[17] Isomorphously doped OMS-2 materials were prepared by refluxing reactant mixtures in the presence of 0.1 M Cu^{2+}, Cr^{3+}, or Ni^{2+} to yield respectively Cu-OMS-2, Cr-OMS-2, and Ni-OMS-2 with dopant levels in the 1–3% range.[23] Undoped OMS-2 was prepared by both the reflux method, K-OMS-2(r), and by calcination of potassium birnessite at 600 °C, K-OMS-2(c).[17]

OMS-2 resistivities were found to be similar for all samples over the temperature range examined. Activation energies were likewise very similar, Table 2. No significant differences were observed between K-OMS-2 and isomorphously doped K-OMS-2, which contrasts the results from OL-1 and OMS-1 measurements. Resistivities of OMS-2 pressed pellet samples (Table 1) exhibited the expected[28] 10^3 increase over single-crystal measurements on K-OMS-2, whereas activation energies were somewhat lower than the 0.76 eV measured for single crystals.[12] Interestingly, OMS-2 resistivities were 2–3 orders or magnitude less than comparable OMS-1 and OL-1 materials despite a general similarity in structure for all three classes of manganese oxides.

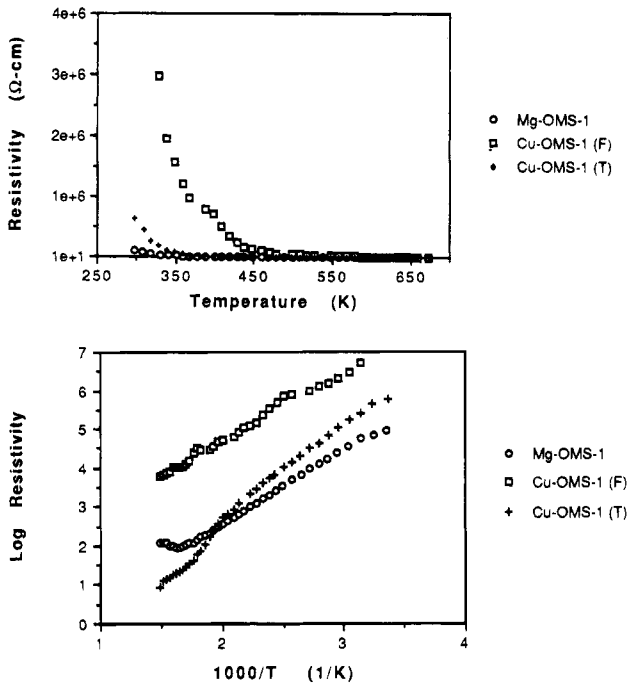

Figure 7. (A, top) Cell resistance of OMS-1 samples from 293 to 673 K. (B, bottom) Arrhenius plots.

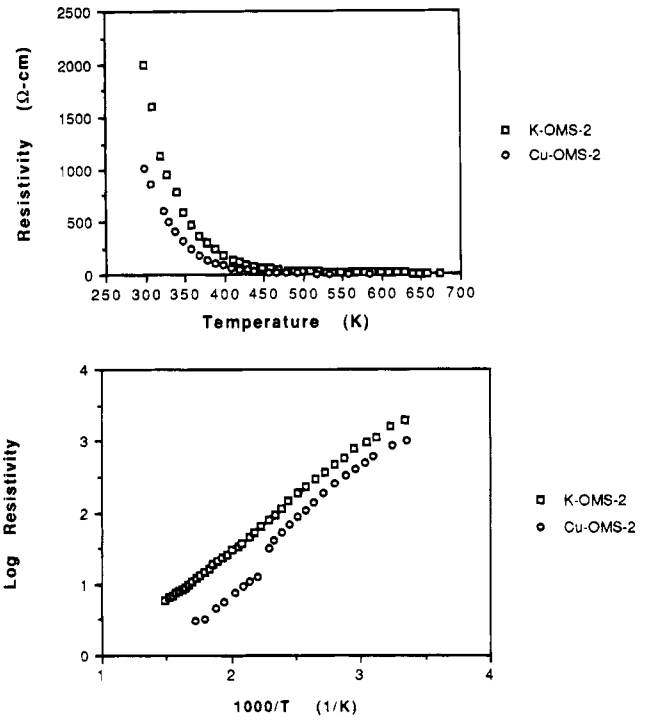

Figure 8. (A, top) Cell resistance of OMS-2 samples from 293 to 673 K. (B, bottom) Arrhenius plots.

High-Temperature Resistivity. Results for the solid-state voltammetry of OMS-1 and OMS-2 showed ohmic responses throughout the temperature range used, 298–673 K. The current–potential plot was linear, and the cell resistance was calculated from the slope. Since the solid-state cell components were identical, the cell resistance was directly related to the manganese oxide disks. The resistivity (ϱ) can be obtained from the resistance of the cell (R) using eq 5,

$$R = \varrho l/A \tag{5}$$

where l is the disk thickness and A the cross section area of the disk. When room-temperature resistivities were calculated using eq 5, the values were 1–2 orders of magnitude larger compared to those obtained by the van der Pauw method. The higher resistivities can be attributed to the higher contact resistance which is inherent in these measurements.

Results of the voltammetric determination of electrical resistance for OMS-1 and OMS-2 samples are shown in Figures 7 and 8, respectively. Both series of samples showed exponential variation in the resistance with increasing temperature. Though the ϱ values obtained from the high-temperature/two-probe method were substantially larger than those measured using the low-temperature/four-probe technique, general differences between OMS-1 and OMS-2 materials remained the same. OMS-1 samples were more resistive compared to OMS-2 samples by 2–3 orders of magnitude. Activation energies for OMS-1 were also slightly higher compared to OMS-2, Table 2.

Cyclic voltammetry (CV) experiments are typically performed in a conductive liquid-phase using electrolyte solutions. Solids are usually studied as modified electrodes. CV methods, however, have been used in the solid phase to study zeolites,[25,26,30] vanadyl sulfate,[31] and molybdenum oxide,[32,33] or to probe electroactive species in conductive polymers.[34] For nonconductive solid substrates such as zeolites, increasing the temperature can enhance the faradaic response of an incorporated electroactive probe molecule. In the solid-state voltammetry studies of manganese oxide samples, no electroactive species were incorporated into the materials. The current–potential plots were ohmic, and the slope provided the resistance of the cell which, in turn, was used to estimate the electrical resistance of the manganese oxides at high temperatures.

After evaluating the data from both the four-probe method at low temperature and the two-probe method at high temperature, it is obvious that while relative comparisons of resistivity and activation energy may have some validity, comparisons of absolute numerical data are unwarranted. The domination of contact resistance in the two-probe method results in a 10^1–10^2 increase over the four-probe method and clearly prevents the two techniques from establishing a contiguous set of data.

Ac Resistivity. Ac resistivity data at 298 K are shown in Table 3 for a representative set of OL-1, OMS-1, and OMS-2 samples. The ac resistivities range from about 10^3 to 10^6 Ω cm. These ac resistivity data show trends similar to the dc resistivity measurements shown in Figures 4–8 and Tables 1 and 2. However, the ac resistivities are generally somewhat larger than the dc values by a factor of 10 at most. We have already pointed out the danger of interpreting dc resistivity data for powdered samples (even pellets) due to grain boundary effects and problems asssociated with the inherent

(30) Creasy, K. E.; Shaw, B. R. *J. Electrochem. Soc.* **1990**, *137*, 2353–2354.

(31) Gorski, W.; Cox, J. A. *J. Electrochem. Soc.* **1992**, *323*, 163–178.

(32) Jaworski, R. K.; Cox, J. A. *Electrochim. Acta* **1992**, *37*, 5–9.

(33) Jaworski, R. K.; Cox, J. A. *Anal. Chem.* **1991**, *63*, 2984–2985.

(34) Wooster, T. T.; Longmire, M. L.; Zhang, H.; Watanabe, M.; Murray, R. W. *Anal. Chem.* **1992**, *64*, 1132–1140.

Table 3. Ac Resistivity Data for Various OL-1, OMS-1, and OMS-2 Samples at 298 K[a]

sample	resistivity (Ω cm)
NaOL-1	5.5×10^6
Cu-OL-1(F)	$>12 \times 10^6$
Cu-OL-1 (L)	$>20 \times 10^6$
Mg-OMS-1	5.4×10^5
Cu-OMS-1(F)	5.5×10^6
Cu-OMS-1(T)	4.9×10^6
K-OMS-2(r)	2.8×10^3
K-OMS-2(c)	$8.2\ 10^3$
CuOMS-2	4.8×10^3

[a] See Table 1 for abbreviations.

assumptions typically used for dc resistivity measurements of single crystals. On the other hand, the ac resistivity data of Table 3 suggest that the trends observed in the dc resistivity data are quite accurate.

Overview

We have previously pointed out that OMS-1, OMS-2, and OL-1 materials have unusual electrical properties[15-18] in addition to their interesting physical properties. Most semiconductors do not show both electrical and paramagnetic characteristics, since the former rely on delocalization of electron density whereas the latter rely on localization of electron density. OMS-1, OMS-2, and OL-1 are reasonably good conductors of electricity and are also of interest because of their paramagnetic properties.[35]

For these samples, the four-probe resistivity measurements are dominated by intergrain boundary resistance. The resistivities reported here are therefore significantly larger than the actual bulk resistivities of these materials. However, it is reasonable to make relative comparisons among the related manganese oxides, especially given their similarities in composition and structure. Such treatment of this type of electrical data is common in the study of conducting polymers.[28]

Several observations indicate that OMS-2 materials are somehow fundamentally different compared to OL-1 and OMS-1 materials in terms of electrical properties. OMS-2 samples are 2–3 orders of magnitude less resistive than OL-1 and OMS-1. Resistivity of OMS-2 samples also exhibits rather conventional variable temperature behavior whereas unusual properties are observed for OL-1 and OMS-1 samples. Finally, OMS-2 appears much less susceptible to resistivity changes due to isomorphous cation substitutions compared to OL-1 and OMS-1. Since all three materials share structural similarities, it appears that this characteristic of the manganese oxides is not responsible for the differences in resistive behavior. Indeed, judging from the solid-state structures shown in Figure 1, it would be more rational to predict similarities for OMS-1 and OMS-2 rather than for OMS-1 and OL-1. One characteristic that does follow the trends in resistivity is the average manganese oxidation state in these materials. All three oxides are mixed valent with respect to manganese, but the degree of mixed valency is not the same in each case. Both OL-1 and OMS-1 contain manganese with an average oxidation state of 3.6, whereas manganese in OMS-2 has an average oxidation state of 3.9.[15-18] If the manganese oxidation states are indeed important to the resistive properties in these materials, it appears that a lower level of mixed valency favors lower resistivity. This may be due to difficulties in electron hopping between sites of low valency which may act as traps.

Conclusions

Electrical resistivities for birnessites (OL-1), todorokites (OMS-1), and cryptomelanes (OMS-2) have been determined by four-probe measurements. The OL-1 and OMS-1 materials have similar properties which differ significantly from the properties of OMS-2 materials. OL-1 and OMS-1 samples had resistivities in the range of 10^5 Ω cm at 298 K and their variable-temperature resistivities deviated from Arrhenius behavior at low temperatures. By contrast, OMS-2 resistivities were in the range of 10^2 Ω cm at 298 K and followed conventional Arrhenius-type activation at low temperatures. Solid-state voltammetry was used to determine the electrical resistance of OMS-1 and OMS-2 at high temperatures. Both materials showed Arrhenius behavior between 293 and 673 K, but contact resistance caused the measured resistivities to be about 1–2 orders of magnitude greater than the values determined by the four-probe method. The semiconducting properties of these layered and tunnel manganese oxides make them interesting materials for battery applications and as potentially useful photocatalysts.[36]

Acknowledgment. We acknowledge the Department of Energy, Office of Basic Energy Sciences, Division of Chemical Sciences and Texaco, Inc., for support of this research. We thank William Zapone and Professor Faquir Jain of the Electrical Engineering Department for help with the ac resistivity measurements.

CM940429N

(35) Suib, S. L.; Iton, L. E. *Chem. Mater.* **1994**, *6*, 429–433.

(36) Cao, H.; Suib, S. L. *J. Am. Chem. Soc.* **1994**, *116*, 5334.